

# SUBGRADE PERFORMANCE ASSESSMENT FOR RIGID RUNWAY USING LONG-TERM PAVEMENT PERFORMANCE DATABASE

Guo-Guang LIU<sup>✉</sup>, Lei-Yang PEI, Zhi-Wei WU

College of Transportation Science and Engineering, Civil Aviation University of China, Tianjin, China

## Highlights:

- a novel method of evaluating subgrade performance was developed and validated using the 726 sets of HWD data;
- statistical analysis demonstrates that the structural behaviour of subgrade follows normal distribution in different service stages;
- the factor analysis show that ATV is the major cause of spatial variations in subgrade condition;
- the aircraft impacts play a positive role in resisting the natural fatigue process by comparison between the main and less trafficked test lines;
- by calculating the effective area of envelope ( $\beta$ ) using the ratio of subgrade performance ( $\eta$ ), it is helpful for airport agency to make decisions scientifically.

## Article History:

- submitted 31 July 2021;
- resubmitted 8 April 2022;
- accepted 24 May 2022.

**Abstract.** Maintaining desired subgrade performance is an effective way to reduce runway pavement deterioration. Due to lack of extensive field test data, life-cycle performance of runway subgrade has not been fully understood. In order to quantitatively estimate subgrade condition, a novel method of evaluating subgrade performance was developed and validated using the 726 sets of Heavy Weight Deflectometer (HWD) test data of ten runway sections. Statistical analysis demonstrates that the structural behaviour of rigid runway subgrade follows normal distribution in different service stages and can be efficiently evaluated by the subgrade performance index ( $\psi$ ). The results of factor analysis show that Accumulated Air Traffic Volume (ATV) during service life is the major cause of spatial variations in subgrade condition. In the designed service period of runway, it validates that sea-reclaimed subgrade results in faster degradation in the initial stage of service life while thicker pavement exhibits better capability in protecting the subgrade soil in long-term view. Besides, the differences in applied loads and pavement thickness give rise to the subgrade performance variation in longitudinal direction. Meanwhile, the comparison between the main and the less trafficked test lines in transversal direction reveals that the aircraft impacts play a positive role in resisting the natural fatigue process. By the suggested method, subgrade performance of HWD test points can be categorized into 4 levels from "Excellent", "Good", "Fair" to "Poor" based on  $\psi$  value. It is helpful for airport agency to make scientific decisions on Maintenance and Rehabilitation (M&R) treatment by calculating the effective area of envelope ( $\beta$ ) using the ratio of subgrade performance ( $\eta$ ).

**Keywords:** rigid runway, subgrade performance assessment, subgrade performance index, long-term pavement performance, heavy weight deflectometer, envelope method.

✉ Corresponding author. E-mail: [ggliu@cauc.edu.cn](mailto:ggliu@cauc.edu.cn)

## Notations

|  |   |
|--|---|
| ACN – aircraft classification number;            | HWD – heavy weight deflectometer;                 |
| AMLW – aircraft maximum landing weight;          | IARC – ICAO aerodrome reference code;             |
| ANN – artificial neural network;                 | ICAO – International Civil Aviation Organization; |
| ASPA – airfield subgrade performance assessment; | LSP – local subgrade performance;                 |
| ATC – air traffic condition;                     | LTRPP – long-term runway pavement performance;    |
| ATV – accumulated air traffic volume;            | ME – Middle East;                                 |
| CBR – California bearing ratio;                  | M&R – maintenance and rehabilitation;             |
| FAA – Federal Aviation Administration;           | NE – North–East;                                  |
| FWD – falling weight deflectometer;              | PCI – pavement condition index;                   |
| GSP – global subgrade performance;               | PCN – pavement classification number;             |
| HA – hub airport;                                | RA – regional airport;                            |

RHA – regional HA;  
SE – South–East;  
SW – South–West;  
TOD – transverse offset distance.

## 1. Introduction

Rigid airfield pavement is by far the most widely used engineering system in Chinese civilian airports. Such system includes several major functional zones, such as runway, taxiway and apron (ICAO 2022). As the increase of the large variety in aircraft types and loads, ATV in recent years, most of the existing researches regarding airfield pavement performance were mainly focused on the bearing capability evaluation based on the internationally adopted comprehensive pavement strength rating system, due to its key relevance to the safety of aircraft landing and take-off (Loizos, Charonitis 2004; White 2017; Liu *et al.* 2020).

This widely accepted evaluation system was developed to protect runway pavement against surface distress and subgrade rutting, by reporting the pavement bearing capacity in terms of the ACN–PCN method (ICAO 2022). In which, PCN is always referred to a specific CBR category while ACN is not affected by the pavement characteristic (Loizos, Charonitis 2004). Consequently, as the development of larger aircraft with higher wheel loads and tyre pressures, the greater pavement dynamic response was observed and higher subgrade support condition degradation was reported (Wang *et al.* 2020, 2015; Dai *et al.* 2003). However, the current aircraft pavement strength rating system was demonstrated to be limited to the subgrade. Hence, in order to make scientific decisions in pavement management practice, subgrade performance evaluation is becoming more and more critical to runway management agencies.

In the design and analysis of rigid pavement system, the multi-layered theory was widely accepted by investigating the interactions of the natural supporting layer, the construct layer and the geometry of the applied loads (Ioannides 1991; Khavassefat *et al.* 2016). With regard to the natural supporting layers, commonly idealized as single materials, the conventional subgrade analysis involved several classical theoretical models using close-form equations, including the Winkler dense liquid model, the Boussinesq elastic solid model, the Pasternak model, the Zhemochkin–Sinityn–Shtaerman model and the Kerr model, etc. (Ioannides 2006).

As the development of modern computers and non-destructive evaluation technologies, more and more alternative but effective methods were developed so as to bridge the gap between theoretical calculation results and field test observations. For instance, FWD, ground penetration radar, surface wave method, 3-dimensional road profiles model, artificial neural network and wireless sensing network, etc., are developed to forward- and back-calculate in-situ subgrade performance of different depths

under various applied loads (Taheri *et al.* 2012; Dong *et al.* 2018; Liu *et al.* 2020; Sangghaleh *et al.* 2014).

However, owing to a lack of reliable calculation model and long-term empirical data, the applied loads and pavement response were more traditionally treated as static and time-independent so as to simplify the computation (Mshali, Steyn 2022). When dynamic impacts of vehicle/aircraft varied with speed was taken into consideration, a novel vehicle-pavement system was proposed to consider the effort of pavement to vehicle by coupling the construct layer and the applied loads (Papagiannakis *et al.* 2007; Snehasagar *et al.* 2020). With quarter car model, half car model, full-car model and various tyre models (Xue, Weaver 2015; Yang *et al.* 2015), the dynamic response between vehicle and multi-layered pavement can be achieved by differential quadrature element method (Rameshkhah *et al.* 2020). Therefore, the dynamic response between the pavement and subgrade, including the distributions of stress, strain and deformation, of subgrade to traffic loads and environment conditions can be accurately obtained (Khoury *et al.* 2022). Under such dynamic impacts of aircraft loads, the mechanical response of subgrade includes both recoverable and irrecoverable deformations (Yang, Cui 2020). This nonlinear damage characteristic of subgrade can cause unpredictable evolution of stiffness degradation and misunderstood of FWD deflection test results of airfield pavement (Rushing *et al.* 2017; Chai *et al.* 2018).

Through road test and full-scale accelerated pavement experiment (Ahmed, Erlingsson 2017), increase in the width of tyre and varying wheel configuration of aircraft gear were proved to induce severe pavement performance deterioration. Therefore, further validation is required at other loading configurations (Gopalakrishnan, Thompson 2006; Xue, Weaver 2015). In spite of this, the transportation industry is still interested in developing larger next generation of aircraft due to economical consideration (Gopalakrishnan 2008). Hence, it is essential to be able to understand the evolution law of subgrade degradation, maintain desired subgrade performance in designed service life under increasing aircraft loads and predict the performance of airport pavements serving the next generation of aircrafts.

There are mainly 2 factors influencing long-term subgrade performance, i.e., the natural fatigue deterioration caused by environmental factors and the external applied loads (Shi *et al.* 2019; Malla, Joshi 2008; Vardon 2015; Feng *et al.* 2018). By full-scale accelerated pavement testing, in-situ assessment and performance analysis (Cunliffe *et al.* 2016; Papadopoulos *et al.* 2016; Park *et al.* 2013), the subgrade fatigue deterioration was proved to be highly depended on the soil physical properties (Alkasawneh *et al.* 2007; Imran *et al.* 2016; Toll *et al.* 2019). Also, the external applied loads had caused the complexity of the stress history and significantly permanent deformations or degradations especially in the somewhat loose subgrade soils (Kim, Tutumluer 2005). In order to characterise the

subgrade performance, resilient modulus ( $M_R$ ) had been widely used as a primary factor for characterising the input parameter of subgrade layer in pavement engineering (Park *et al.* 2013). Based on the mechanistic-empirical theory, repeated tri-axial load test, pavement deflection test and numerical simulation, etc., different methods had been established to measure or estimate  $M_R$  varied within subgrade layer, and the results were in correlating laboratory  $M_R$  to stress state (Rahim, George 2005; Alkasawneh *et al.* 2007). Recommend stating that HWD was the most commonly used in-situ method for determining  $M_R$ .

Despite all the investigations performed on  $M_R$  prediction, it still remains a great challenge to describe the evolution law of subgrade deterioration in long-term view. Similar to the dynamic impacts of vehicle on road pavement, the aircraft load can be decomposed into static load, 2-fold dynamic load and roughness-dependent load with a 4-fold increasing coefficient (Lin 2014). When the upward wing-lift force is taken into consideration, the dynamic load of aircraft on runway pavement varies obviously during different landing period, such as touch-down period, deceleration period and taxiing period. Then, different vertical inertial forces are transmitted through the suspension system and wheels to the pavement and finally to the subgrade soil. Therefore, the energy transfer differences from aircraft to subgrade soil is the main cause of  $M_R$  variation. Then, the subgrade performance in different runway functional zones is highly related to the external energy input. Similar phenomenon had also been observed in the vibration compaction process during subgrade construction. The compaction performance depends upon not only the materials but also the construction procedure. In which, the latter are mainly associated with the contact force and the vibration frequency (Jia *et al.* 2020). Lower subgrade condition means less compaction energy absorbed from vibrator.

In order to explain the evolution laws of subgrade degradation in life-cycle, Miner's fatigue law was widely applied in the practice of runway pavement management (Ioannides 2006). Although it is high efficiency to predict the remained service life by counting the passing numbers of aircraft, it still remains a problem for airport agency to scientifically evaluate the subgrade deterioration degree and appropriately adopt M&R measures such as the surface functionality controlling in researches of Biancardo *et al.* (2020) and De Luca *et al.* (2016). If the back-calculated  $M_R$  from HWD is underestimated, M&R decisions may not be economical (El-Raof *et al.* 2020). Therefore, there is a need to explore the evolution law of subgrade deterioration of many factors in designed life-cycle.

To address this need, the primary objective of this study is to develop a rapid and reliable evaluation method, so as to provide a good assessment of long-term subgrade performance, without complex process of finite element analysis. For these objectives, ASPA method was proposed for subgrade characteristic analysis based on

Chai and Kelly's Equation and measured deflection data of in-service rigid pavement. Then, the subgrade behaviour of rigid runway was studied by typical sections of HWD test extracted from LTRPP database so that the life-cycle evolution trend of subgrade deterioration obtained from the evaluation model can be statistically analysed. Moreover, the variations of subgrade performance in transverse and longitudinal directions were investigated to explain the spatial distribution of subgrade deterioration under several factors, i.e., service life, layer property, ATC, etc. The outcomes of this work are helpful for runway management agencies to efficiently identify the location of severe subgrade deterioration and make scientific decisions on M&R. Also, the following design control method can be improved according to the environmental characteristics of different areas.

## 2. Development of the methodology

### 2.1. Chai and Kelly's Equation

By investigating FWD data from LTPP, Chai & Kelly (2008) found that the FWD deflection bowls were well matched by exponential curve, as shown in equation:

$$Y_r = K_1 \cdot e^{\left(\frac{-r}{K_{2,r}}\right)}, \quad (1)$$

where:  $Y_r$  is the FWD deflection at the respective sensor location;  $r$  is the respective sensor offset location;  $K_1$  is equal to deflection at  $D_0$  in sensor;  $K_{2,r}$  is the structural parameters at the respective sensor location.

Besides, Chai *et al.* (2018) also found that the linear and nonlinear behaviours of subgrade can be characterized by the deflection ratio ( $DefR$ ). One interesting aspect of the  $DefR$  method is that the ratios are observed to be <2 for pavements with linear subgrade. As show in below equation,  $DefR$  is defined as the ratio of the FWD deflection of a sensor divided by the deflection of the preceding sensor:

$$DefR_i = \frac{D_i}{D_j}, \quad (2)$$

where:  $D_i$ ,  $D_j$  are the FWD deflections at sensor locations  $i$  and  $j$ , respectively,  $i = 1, 2, 3, \dots, 8$ ,  $j = i + 1$ .

By Equation (1) and (2), we can reach to the following equation for  $DefR$ :

$$DefR_i = e^{\frac{r_j}{K_{2,rj}} - \frac{r_i}{K_{2,ri}}}. \quad (3)$$

The derived expression is suitable for interpreting the variations of deflection basin curve and structural performance of both flexible and rigid pavements. By which, Chai *et al.* (2018) validated the nonlinear performance of subgrade in flexible pavement. However, the subgrade behaviour of rigid pavement has not been investigated by  $DefR$  until now.

## 2.2. ASPA

In order to evaluate the subgrade deterioration condition of rigid runway pavements, subgrade performance index ( $\psi$ ) was developed based on Chai and Kelly's equation (Chai, Kelly 2008)), as shown by equation:

$$\psi_a = \frac{K_{2,900}^a}{K_{2,average}^a}, \quad (4)$$

where:  $a$  is the number of HWD test point;  $K_{2,900}^a$  is the structural parameter of the  $a$ th test point as defined in Equation (1);  $K_{2,average}$  is the average value of the investigated  $K_{2,900}^a$ .

To eliminate the influence of pavement thickness on  $\psi$  (Chai et al. 2018), the subgrade structural parameter ( $K_{2,900}$ ) in this work was determined by the deflection at  $D_{900}$ . When the  $K_{2,900}$  is within the range from 100 to 300, it is associated with high degree of subgrade nonlinearity. For moderate degree of nonlinearity,  $K_{2,900}$  falls within the range between 300 and 500. Then, the LSP and the GSP can be estimated by choosing proper  $K_{2,average}$ . If  $K_{2,average}$  stands for the average value of a section,  $\psi$  represents the subgrade condition of the specific runway. When  $K_{2,average}$  represents the average value of several runways,  $\psi$  reflects the relative subgrade condition between investigated runways.

By ASPA, subgrade performance can be categorized into different levels by defining proper threshold values of  $\psi$ . And the proportion of each level can be described by the ratio of subgrade performance ( $\eta$ ) in equation:

$$\eta = \frac{n}{N} \cdot 100\%, \quad (5)$$

where:  $n$  is the total number of  $\psi_a$  classified in the same level;  $N$  is the total number of test points.

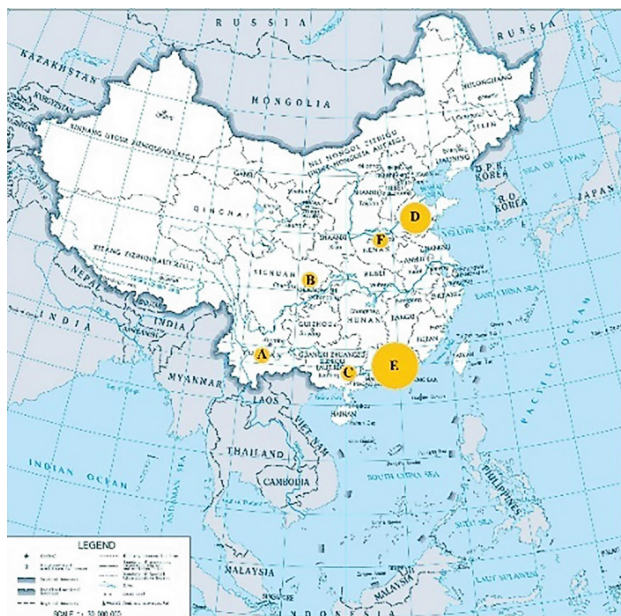


Figure 1. Locations of airports selected from LTRPP database

While the process to determine  $M_R$  is time-consuming if done directly using the finite element method, the subgrade stiffness condition can be evaluated instantly via the proposed ASPA method. Then, the subgrade performance of HWD test point can be quantitatively described and compared in efficiency.

## 3. Description of the experimental research

To analyse the above proposed ASPA, ten sections of rigid runway with 726 sets of HWD test point were extracted from LTRPP database established by a research institution of China, as shown by Figure 1. At each HWD test point, 9 deflection values were measured for analysing the behaviour of subgrade performance in rigid runway (Liu et al. 2020), as shown by Figure 2. These sections were selected such that they covered 4 major geographical regions in China with typical ICAO IARC, ATC and service life, etc., as listed in Table 1.

## 4. Results and discussions

### 4.1. Subgrade behaviours of rigid runway

#### 4.1.1. Characteristic of deflection bowl

Figure 3 compared 25 sets of deflection basin data of HWD test selected from the main landing zone and the taxiing zone, respectively. It can be seen that the 4th order equation fitted the measured deflection bowl of rigid pavement very well ( $R^2 > 0.9$ ). Besides, both the minimum and maximal deflection bowls in the main landing zone (with designed thickness of 42 cm) were smaller than that in the taxiing zone (with designed thickness of 38 cm). Greater deflection variation ranges of  $D_0$  (114.34  $\mu\text{m}$ ) in

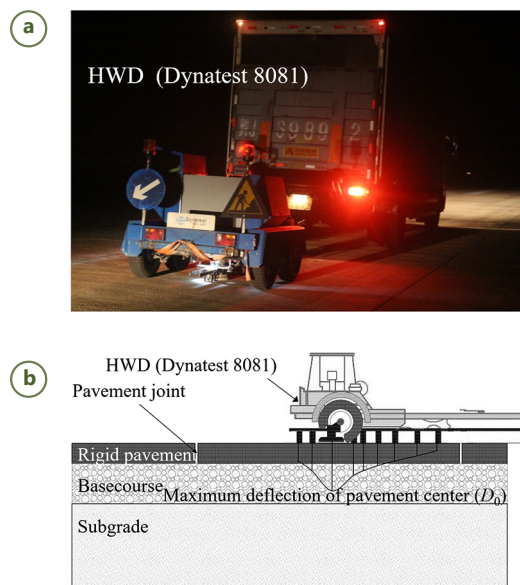
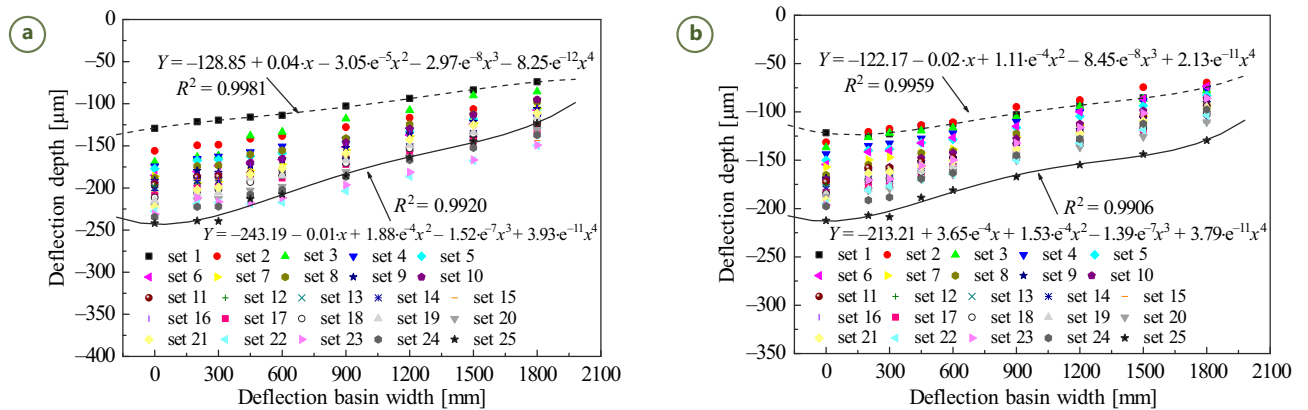


Figure 2. HWD test:

(a) – field test; (b) – sensors layout of HWD

**Table 1.** Characteristics of rigid runway sections of the selected airports

| Section ID | IARC | Length [m] | ATC | Location | No of test points | Service life [year] | Subgrade type |
|------------|------|------------|-----|----------|-------------------|---------------------|---------------|
| A          | 4C   | 2500       | RA  | SW       | 62                | 15                  | normal        |
| B          | 4C   | 2500       | RA  | SW       | 62                | 20                  | normal        |
| C          | 4C   | 1800       | RA  | SW       | 35                | 25                  | normal        |
| D1         | 4D   | 3200       | RA  | NE       | 81                | 5                   | normal        |
| D2         | 4E   | 3400       | HA  | NE       | 81                | 5                   | normal        |
| E1         | 4F   | 3600       | HA  | SE       | 81                | 15                  | normal        |
| E2         | 4E   | 3600       | HA  | SE       | 81                | 20                  | normal        |
| E3         | 4E   | 3400       | RHA | SE       | 81                | 23                  | sea-reclaimed |
| F1         | 4E   | 3400       | RHA | ME       | 81                | 29                  | normal        |
| F2         | 4E   | 3400       | RHA | ME       | 81                | 29                  | normal        |



**Figure 3.** Typical deflection basin shape on zones of section F1 under serving 29 years:

(a) – taxiing zone; (b) – main landing zone

the taxiing zone indicates its subgrade condition deteriorated more significantly than the main landing zone. This proves that the measured deflection bowl is profoundly affected by the pavement thickness. After 29 years of service, thicker pavement of the main landing zone still plays a better role in protecting subgrade soil than the taxiing zone with pavement thickness reduction under the same applied loads.

**4.1.2. Variation of subgrade structural behaviour**

In order to verify the existence of equivalence relation between deflection variations and subgrade stiffness,  $DefR$  and  $K_{2,900}$  were calculated for all test points using Equations (1) and (2). Table 2 summarized and compared ten typical deflection curves with maximum  $D_0$  in respective section. It can be seen that the maximum value of  $DefR$  is less than 2 and minimal value of  $K_{2,900}$  is greater than 500, which demonstrates that the subgrade performance of rigid runway shows linear behaviour (Chai *et al.* 2018).

To achieve greater efficiency in comparing subgrade structural behaviour between different sections,  $K_{2,average}$  of each selected section was also summarized in Table 2. It can be seen that the increasing service life will produce lower  $K_{2,average}$  in HA, however this trend is not true for RA and RHA. It indicates that  $K_{2,average}$  can be a proxy to evaluate subgrade stiffness, but does not provide ad-

equate information about the evolution law of subgrade performance affected by ATC.

Furthermore, in order to investigate the distribution law of subgrade behaviour, typical curves of  $DefR_5$  distributed in runway longitudinal direction were presented by Figure 4. In general, there is a random increase of  $DefR_5$  values as the growth of service life both in RA and HA. In particular, the increase of  $DefR_5$  in the main landing zone is faster than that in the secondary landing zone. It reflects that the combined impacts of service life and ATC play key roles in the long-term evolution of subgrade behaviour. Further analysis on subgrade structural performance is still required.

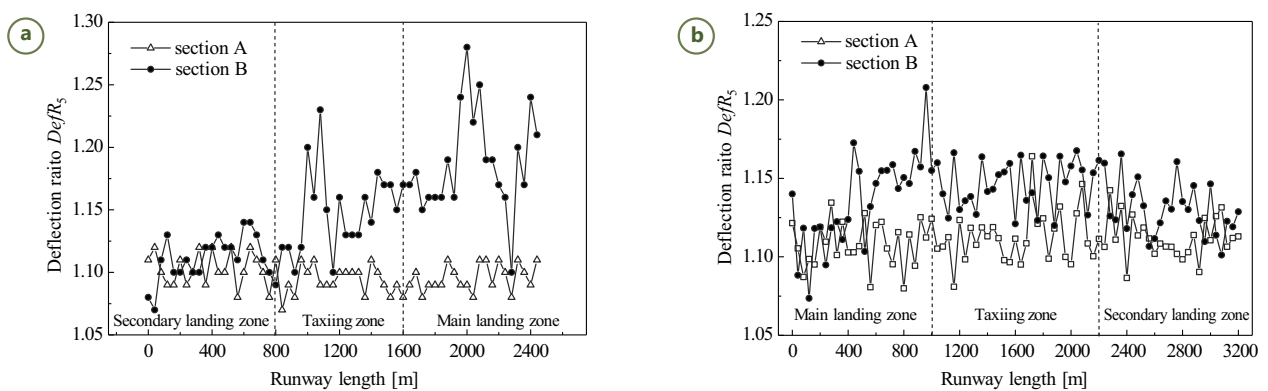
**4.1.3. Statistical analysis of subgrade performance**

As analysed above, almost each test point of the section exhibits a different stiffness condition. In practice, it is hardly to obtain the historical value of  $K_{2,average}$  for a runway in life-cycle due to lack of continuous HWD test data.

Since the cumulative damage of subgrade is dramatically influenced by magnitude and frequency of repeated aircraft loads, 3 sections of HA, with similar geometry and ATC but different service life, were extracted from LTRPP database (Table 1). In order to obtain a stable estimation, subgrade performance of sections D2, E1 and E2 were investigated statistically by analysing the variation of  $K_{2,900}$  in this work.

**Table 2.** Sample calculations for different HWD test sections

| Section ID | Maximum value of $D_0$ | DefR     |          |          |          |          |          |          | $K_2, 900$ | $K_2, average$ |
|------------|------------------------|----------|----------|----------|----------|----------|----------|----------|------------|----------------|
|            |                        | $DefR_1$ | $DefR_2$ | $DefR_3$ | $DefR_4$ | $DefR_5$ | $DefR_6$ | $DefR_7$ |            |                |
| A          | 335.4                  | 1.38     | 1.03     | 1.07     | 1.07     | 1.11     | 1.13     | 1.13     | 1522       | 3391           |
| B          | 556.7                  | 0.95     | 1.05     | 1.22     | 1.09     | 1.17     | 1.20     | 1.21     | 2048       | 2508           |
| C          | 428.1                  | 1.33     | 1.04     | 1.07     | 1.10     | 1.17     | 1.19     | 1.21     | 1397       | 2893           |
| D1         | 169.9                  | 1.05     | 1.02     | 1.11     | 1.07     | 1.14     | 1.15     | 1.14     | 2422       | 3176           |
| D2         | 119.8                  | 1.09     | 1.03     | 1.16     | 0.98     | 1.17     | 1.13     | 1.16     | 2245       | 3193           |
| E1         | 149.4                  | 1.05     | 1.03     | 1.15     | 1.08     | 1.16     | 1.19     | 1.18     | 2030       | 2939           |
| E2         | 213.5                  | 1.06     | 1.02     | 1.15     | 1.09     | 1.21     | 1.28     | 1.33     | 1820       | 2435           |
| E3         | 259.7                  | 0.96     | 1.26     | 1.03     | 1.16     | 1.19     | 1.20     | 1.17     | 1660       | 3339           |
| F1         | 234.6                  | 1.06     | 1.00     | 1.07     | 1.03     | 1.08     | 1.12     | 1.10     | 3872       | 3852           |
| F2         | 319.7                  | 1.06     | 1.01     | 0.97     | 1.02     | 1.04     | 1.07     | 1.07     | 4215       | 3444           |

**Figure 4.** Typical curves of  $DefR_5$  for airports: (a) – RA; (b) – HA

As presented in Figure 5, the shape of normal distribution curve of  $K_{2, 900}$  is substantially affected by the expectation value ( $\mu$ ) and the variance value ( $\sigma$ ). It demonstrates that  $\mu$  represents the estimated value of subgrade stiffness with the maximum probability, and  $\sigma$  describes the variation range of subgrade performance. It is of interest that, the maximum probability value of  $K_{2, 900}$  was increased while the value of  $K_{2, average}$  was decreased with the growth of service life. Therefore, the variations of  $K_{2, 900}$  in different service life were proved to be consistent with the normal distribution well enough to be used to categorize subgrade performance by inverse analysis.

#### 4.1.4. Probabilistic categorisation of subgrade performance

Based on the successful establishment and validation of ASPA method, an evaluation matrix can be developed to identify subgrade performance by different ranges of  $K_{2, 900}$ . As illustrated by Figure 6, the subgrade performance can be divided into 4 categories from "Excellent" to "Poor" according to the probabilistic value of  $K_{2, 900}$ . In which,  $K_{2, average}$ ,  $K_{2, low}$  and  $K_{2, up}$  were defined as the threshold values to quantitatively determine subgrade performance.

As mentioned above, when investigating LSP of a section,  $K_{2, average}$  is a constant determined by HWD test result directly. While comparing GSP of several runways,

$K_{2, average}$  is assigned to be the average value of  $K_{2, 900}$  in all sections. Then,  $K_{2, low}$  and  $K_{2, up}$  can be solved by assigning different probabilistic values to each categorization using equation:

$$P(K_{2, low} \leq x \leq K_{2, up}) = \int_{K_{2, low}}^{K_{2, up}} \frac{1}{\sqrt{2\pi}\sigma} \cdot e^{-\frac{(x-\mu)^2}{2\sigma^2}} dx, \quad (6)$$

where:  $K_{2, low}$ ,  $K_{2, up}$  are the independent normal random variables.

For section with  $K_{2, 900}$  less/greater than  $K_{2, low} / K_{2, up}$ , the subgrade performance was classified as "Poor"/"Excellent". In contrast, if  $K_{2, low} \leq K_{2, 900} \leq K_{2, up}$ , the subgrade performance was in "Fair"/"Good" condition, respectively.

As present in Table 3, multiple comparisons between different intervals of  $\psi$  were conducted to determine how they varied with the probabilistic value of subgrade performance. Based on our best knowledge from runway evaluation, the probabilistic value for "Excellent", "Good", "Fair" and "Poor" are suggested to be 5.0, 45.0, 50.0 and 10.0% respectively, as summarized in Table 4. It should be noted that RHA was sorted into RA due to their similarity in the standard of runway pavement design and construction.

Then, Figure 7–12 were plotted to assess the effects of various parameters on the evolution of subgrade degradation, including layer property, service life and ATC.

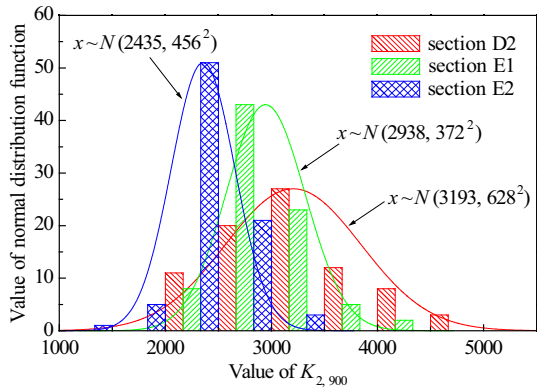


Figure 5. Normal distribution curves of  $K_{2,900}$

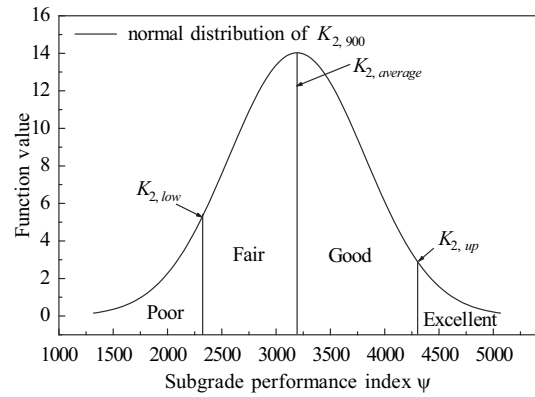


Figure 6. Sample of probabilistic categorisation for ASPA

Table 3. Calculated interval of  $\psi$  under different probabilistic values

| Section ID | Calculated interval of $\psi$ |              |              |              |
|------------|-------------------------------|--------------|--------------|--------------|
|            | $P = 60.0\%$                  | $P = 70.0\%$ | $P = 80.0\%$ | $P = 90.0\%$ |
| A          | [0.89, 1.11]                  | [0.86, 1.14] | [0.83, 1.17] | [0.78, 1.22] |
| B          | [0.73, 1.27]                  | [0.67, 1.33] | [0.59, 1.41] | [0.48, 1.52] |
| C          | [0.74, 1.26]                  | [0.68, 1.32] | [0.60, 1.40] | [0.49, 1.51] |
| D2         | [0.83, 1.17]                  | [0.80, 1.12] | [0.75, 1.25] | [0.68, 1.32] |
| E1         | [0.89, 1.11]                  | [0.87, 1.13] | [0.84, 1.16] | [0.79, 1.21] |
| E2         | [0.84, 1.16]                  | [0.80, 1.20] | [0.76, 1.24] | [0.69, 1.31] |

Table 4. Categorisation of subgrade performance by  $\psi$

| Subgrade performance | Probabilistic value | Range of $\psi$ |              |
|----------------------|---------------------|-----------------|--------------|
|                      |                     | RA              | HA           |
| Excellent            | <5.0%               | [1.50, +∞)      | [1.30, +∞)   |
| Good                 | >45.0%              | [1.00, 1.50]    | [1.00, 1.30] |
| Fair                 | >40.0%              | [0.60, 1.00]    | [0.75, 1.00] |
| Poor                 | <10.0%              | [0, 0.60]       | [0, 0.75]    |

## 4.2. Influence of layer property on subgrade performance

As a multi-layered system, we are interested in 2 basic properties of pavement: the pavement thickness of construct layer and the properties of subgrade material.

### 4.2.1. Pavement thickness

Pavement thickness is an important design factor affecting the long-term subgrade performance and protecting subgrade against deterioration. Thicker concrete slab leads to less stress response of subgrade soil under the same external applied loads. However, during the runway pavement design, the slab thickness in the middle part (taxiing zone) is reduced on purpose from economical consideration. Hence, the research on the relationship between pavement thickness and  $\psi$  plays a key role in understanding the evolution law of subgrade deterioration.

As a typical HA with balanced arrival-departure aircrafts, section E2 is the best example in LTRPP database to investigate the impact of pavement thickness on subgrade degradation. Figure 7 shows the curve of  $\psi$  varied

in longitudinal direction of runway. It can be seen that the maximum and minimal value of  $\psi$  were found in the 2 landing zones (0.97 and 0.94) and the taxiing zone (0.42), respectively. Also, the average value of  $\psi$  for 2 landing zones (0.75) is greater than that of the taxiing zone (0.68). This indicates that the subgrade condition gradually decreased from runway end to runway centre under repeated aircraft landing weight for 20 years. Besides, the subgrade performance of the taxiing zone turns out to be the worst among all test points due to its pavement thickness reduction design. As for the main and secondary landing zones with equal thickness and balanced ATC, there is a similar trend of subgrade deterioration only with slight differences in  $\eta_{poor}$  and the minimal value of  $\psi$ . Therefore, the long-term subgrade performance is proved to be sensitive with the pavement thickness.

The maximum value of  $\psi$  in section E2 is less than 1.0 because  $K_{2,average}$  was assigned to be the average value of  $K_{2,900}$  for all selected sections of RHA and HA as listed in Table 1. It is fairly clear from Figure 7 that GSP of section E2 is relatively worse compared with the average performance.

#### 4.2.2. Subgrade type

It is well known that settlement of subgrade soil would lead to long-term geometry degradation. Hence, the subgrade type is another key factor affecting subgrade behaviour. In order to understand its influence on subgrade degradation, 2 sections (E3 and F1), with same IARC and similar ATC but different subgrade type, are selected to investigate the subgrade deterioration trend.

Figure 8 compared the calculated  $\psi$  between section E3 and section F1. For the rigid runway overlay on the normal ground, the values of  $\eta$  from "Excellent" to "Poor" were 12.4, 44.4, 35.8 and 7.4%, respectively. As for the sea-reclaimed subgrade, 96.3% of the subgrade are ranked as "Good" and "Fair". With shorter service life, subgrade performance of section E3 demonstrates that greater settlement of reclaiming ground in the initial service stage has resulted in faster degradation than the natural ground. As time passes, the subgrade settlement tends to be stable and the runway subgrade is still "Fair" enough for safety operation. This is also justified by the results of periodical settlement observation and pavement condition evaluation carried out by airport management agency.

#### 4.3. Influence of service life on subgrade performance

It is absolutely true that the subgrade condition will change with service life. However, it is still unclear how these changes are influenced by service life. With typical airports select from LTRPP database, the influence of service life on subgrade performance is analysed by comparing 3 HA sections and 3 RA sections.

##### 4.3.1. HA

Figure 9 showed the variation curves of  $\psi$  in runway longitudinal direction of 3 HAs with different service life. It can be seen that increasing of the service life results in decreasing the subgrade performance. For instance, the sum of estimated "Fair" and "Poor" subgrade conditions of 3 sections, with 5, 15 and 20 years of service, are 58.0, 85.2 and 100.0%, respectively.

Generally, in the initial stage of service (5 years), the subgrade behaviour is varied randomly and mainly affected by construction quality. In the 1st 15 years, the subgrade deteriorations in 2 runway ends, both in landing and take-off phases of aircrafts, are severer than the rest part of runway. When it reaches to 20 years, the subgrade settlement is stable and the subgrade performance is highly sensitive with pavement thickness. However, pavement thickness reduction design dramatically speeds up the subgrade degradation in the taxiing zone. As a result of this analysis, it can be interpreted from Figure 9 that the critical service life of subgrade degradation was found to be between 15 to 20 years, which is agreed with our previous ANN predictions on the runway pavement performance (Liu *et al.* 2020). And, study has found that the transfer mechanism of road-soil foundation energy

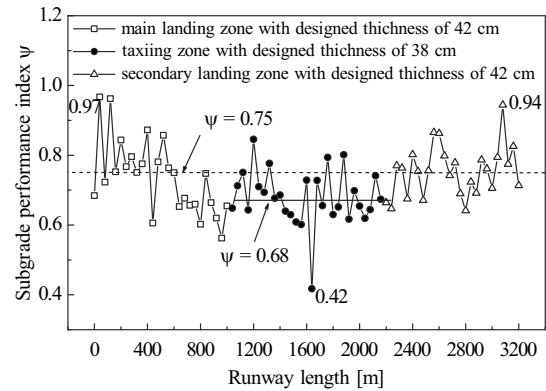


Figure 7. Variations of calculated  $\psi$  for test section E2

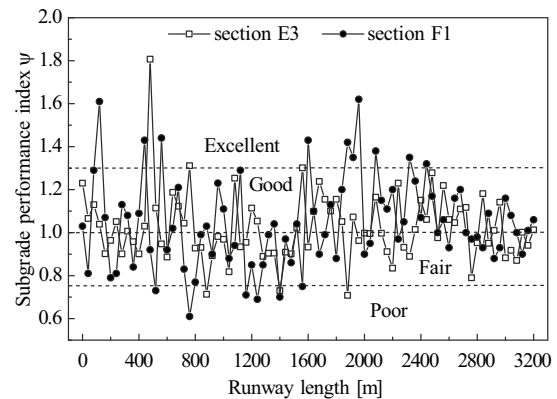


Figure 8. Variations of  $\psi$  for test sections E3 and F1

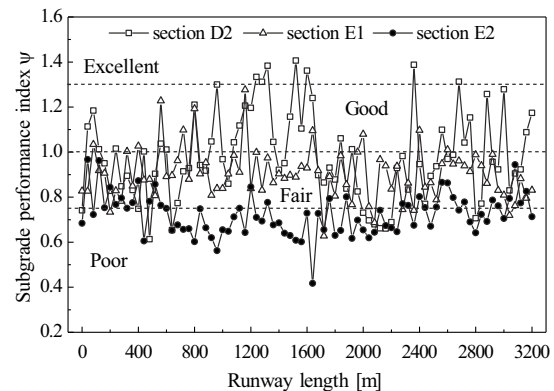


Figure 9. Variations of  $\psi$  for HA

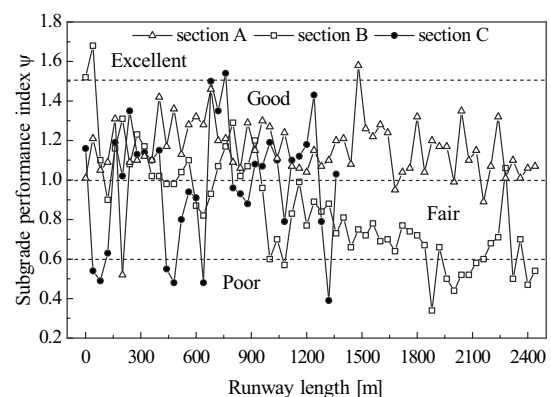


Figure 10. Variations of  $\psi$  for RA

mainly depends on the parameters of subgrade, and the concrete structure only affects this in a small range with a high frequency, similar to Lak *et al.* (2011). Then, proper M&R treatment should be conducted in this period so as to relieve the subgrade degradation trend and prolong runway service life.

**4.3.2. RA**

Similarly, Figure 10 compared the subgrade performance of 3 RAs with different service life. After 15 years of service, “Good” subgrade performance was still dominated in section A. It indicates that for RA, which has shorter runway length and lighter AMLW, the evolution process of subgrade deterioration is slower than HA. Besides, it is of interest that, one-way landing and take-off strategy results in unbalanced evolution of subgrade deterioration in section B. In which, the calculated  $\eta_{Poor}$  of the main-landing zone is around 16.0% while the other runway end still remains in “Good” and “Fair” condition. Also, it is most likely the reason of unusual rate of “Good” performance in section C, which owns the shortest runway length, lightest AMLW and lowest ATV.

In consequence, our analysis demonstrates that the evolution of subgrade deterioration of HA is highly dependent on service life and, furthermore, that the reduction in pavement thickness leads to faster deterioration at the late stage of service life. Compared with HA, the evolution of subgrade deterioration in RA is mainly controlled by the actually applied loads. With balanced arrival-departure aircrafts, RA shows strong ability in maintaining “Good” subgrade condition and requires less repairment in designed service period. In other special scenarios, severe deterioration of subgrade is mainly caused by ATC.

In general, the above calculated results imply that the deterioration rate of subgrade in HA is faster than RA. Furthermore, close attentions should also be paid to the thickness reduction segments of both HA and RA, especially in the late stage of designed service period, so as to make scientific decisions on M&R treatment and prolong the service life. And statistical analysis can provide reference for the design of airport runway in environmentally analogous regions.

**4.4. Influence of ATC on subgrade performance**

As discussed above, ATC is a major factor in relate with subgrade deterioration. To understand its impacts on subgrade performance, the influences of 2 key factors should be considered during ASPA, namely, ATV and TOD.

**4.4.1. ATV**

According to Miner’s fatigue law, the remained service life of runway is determined by the actual passing number of standard aircraft (Aydin, Topal 2019). Hence, the subgrade performance is highly related to ATV. Variation curves of  $\psi$  for sections D1 and E1, with different ATV, are compared in

Figure 11. As expected, the general subgrade performance decreased with increasing service life. It is interesting to note that the values of  $\eta_{Excellent}$  in both sections are consistent (zero) according to the threshold values suggested for HA and RA in Table 4, respectively. In addition, the value of  $\eta_{Poor}$  in section E1 is 7.4% while that of section D1 is still zero. The results demonstrate that severer subgrade degradation in section E1 is caused by higher ATV and also indicate it is in the critical stage of subgrade deterioration as  $\eta_{Excellent}$  is zero and  $\eta_{Poor}$  is close to 10.0%. Therefore, it is of efficiency to quantitatively evaluate the influence of ATV on subgrade degradation by ASPA.

**4.4.2. TOD**

TOD was defined as the distance between runway central line and HWD test section. During runway pavement evaluation, TOD is determined by the major main gear configurations of commercial aircraft from economic considerations. In order to further understand the influence of aircraft impacts on subgrade condition, a comparing HWD test was carried out on the same runway in section F1 with TOD of 2.25 m and section F2 with TOD of 6.75 m.

Figure 12 shows an unexpected decrease of subgrade performance in the less trafficked zone (section F2) compared with the main trafficked zone (section F1). In section F2,  $K_{2, average}$  is 10.6% less than section F1, which implies high sensitivity of subgrade performance to TOD. The subgrade performance in section F2 is essential to aircraft safety due to it directly supports the main gears of heavier aircraft, such as A380, B747, etc. However, most researchers and pavement managers pay less attentions to this phenomenon.

In addition, the main trafficked zone shows greater  $\eta_{Excellent}$  than the less trafficked zone. It indicates that the repeated aircraft load plays a positive role in resisting natural fatigue by compacting subgrade soil. Also, the greater in  $\eta_{Poor}$  of section F1 validates the significant influence of ATC on subgrade deterioration as mentioned above. Benefit from the safety margin during the runway geometry design, the subgrade performance of section F1 is still “Fair” enough for operation at the last year of designed service life.

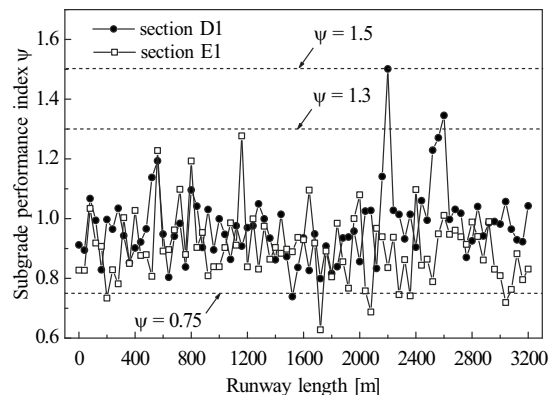


**Figure 11.** Variations of  $\psi$  for test sections D1 and E1

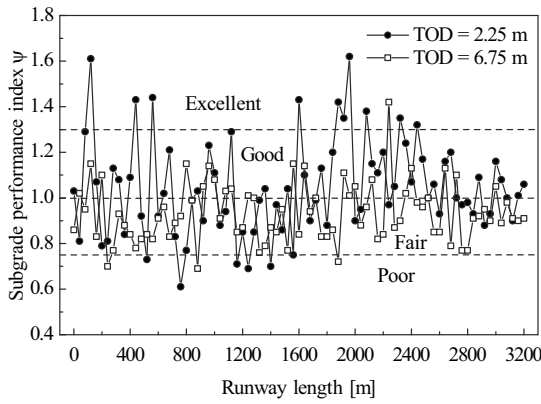


Figure 12. Variations of  $\psi$  in different test lines for test section F

#### 4.5. Envelope method for M&R decisions

It is evident that the subgrade performance is varied in each test point with service life, ATC and locations. At project level,  $\psi$  information can be used as an indicator to locate "Poor" subgrade condition and make proper maintenance decisions on pavement segment. However, it is not recommended as a decision-making tool for the rehabilitation of rigid runway due to  $K_{2, average}$  might underestimate/overestimate the subgrade performance of landing/taxiing zone. In order to obtain more definitive and quantitative guidelines for M&R decision, an envelope method to statistically and quantitatively evaluate the general subgrade performance of the entire runway is developed based on the successful application of ASPA.

As shown by the radar map of Figure 13, the subgrade performance envelope is formed by 4 straight lines connecting different values of  $\eta$  at each axis. The envelope shape can represent all complex subgrade conditions affected by many factors. In order to reflect the negative effects of "Poor" subgrade performance, the areas in the 2nd and the 3rd quadrant are assigned to be negative. Therefore, the effective area of envelope ( $\beta$ ) can be calculated by an empirical function of equation:

$$\beta = \frac{(\eta_{Fair} + \eta_{Good}) \cdot (\eta_{Excellent} - \eta_{Poor})}{2} + 0.05. \quad (7)$$

It can be seen that, if  $\eta_{Excellent} = 5.0\%$ ,  $\eta_{Good} = 45.0\%$ ,  $\eta_{Fair} = 40.0\%$  and  $\eta_{Poor} = 10.0\%$ , as suggested in Table 4,  $\beta$  is equal to 0.03. Hence, it is defined as the statistically critical phase of subgrade performance. When  $\beta$  is greater/less than 0.03, the subgrade performance is defined as the 1st/2nd phase.

By this envelope method, the evolution of subgrade performance can be described as the decreasing process of  $\beta$  from the 1st phase (greater than 0.03) to the critical and 2nd phase (less than 0.03). The calculated value of  $\beta$  for previous discussed sections are listed in Figure 14. The runway management authority can correctly understand the performance of the runway foundation based on the values of  $\beta$ , so as to make scientifically appropriate airport maintenance and repair decisions.

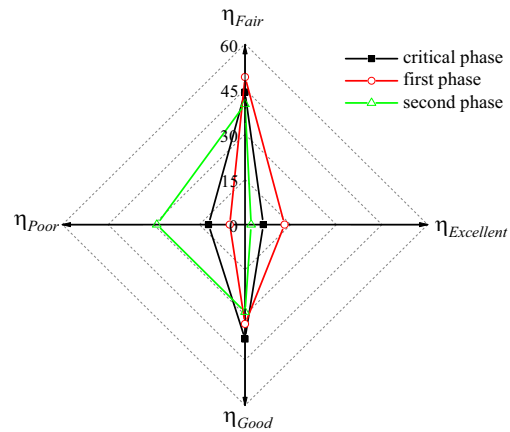


Figure 13. Typical envelope of subgrade performance

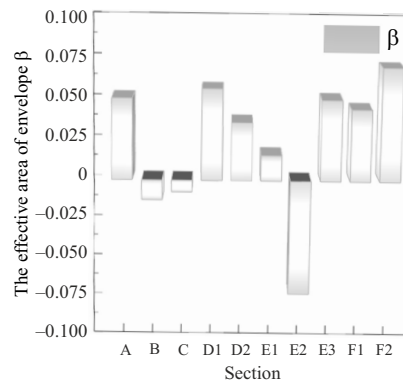


Figure 14. Calculated value of  $\beta$  for selected sections

It can be seen that, GSP can be quantitatively compared by the value of  $\beta$  between different runways regardless of influencing factors. It demonstrates that the envelope method can be a simple and yet a powerful approach for airport management agency to conduct ASPA, so as to scientifically make appropriate M&R decisions. During the M&R of these airport runways, experience can be gained in the design of runways at other airports in the region.

## 5. Conclusions

An alternative method for evaluating subgrade performance of rigid runway had been developed based on Chai and Kelly's Equation. The proposed ASPA method derived in this work was used to investigate the influence of a variety of factors on the structural behaviour of runway subgrade using measured HWD test data extracted from LTRPP database. By considering the long-term influence of service life, ATC and layer properties, etc., further analysis was conducted to investigate the evolution law of subgrade condition by  $\psi$ , identify subgrade deterioration condition by  $\eta$  and evaluated GSP by  $\beta$ . With different threshold values of  $\psi$  inverse-calculated from the normal distribution function, the subgrade performance of each HWD test point was categorized into 4 levels from "Excellent" to "Poor".

It is found that the subgrade structural performance of rigid runway shows linear behaviour under applied loads and varies in normal distribution along runway. As the growth of service life, the subgrade performance is mainly associated with the pavement thickness and ATC. In general, the spatial distribution of subgrade performance was found to be irregular and discrete. In particular, severer subgrade deteriorations were observed in the taxiing zone of HA and the landing zone of RA in long-term view.

However, the usual “average-based” evaluation of subgrade performance, i.e.,  $K_{2, average}$ , is found to be incapable in deciding proper M&R actions due to its potential great error caused by the combined natural fatigue process and random aircraft impact. Instead, an envelope method was suggested to predict subgrade performance quantitatively by calculating the value of  $\beta$  based on the radar map of  $\eta$ .

In worldwide, the construction and operation of runway pavement are strictly regulated by the rules of FAA and ICAO. Therefore, the evaluation of runway pavement deterioration follows a similar pattern by analysing LTRPP database, such as the variations of PCI and PCN. In this work, the changes of subgrade performance in life-cycle are not limited to specific weather conditions, the specifics of aviation, and runway pavements of a specific structure of China.

Therefore, the proposed ASPA method is proved to be high efficiency in identifying different deterioration conditions of a particular pavement segment, comparing general subgrade performance between different sections and predicting the subgrade performance of any runway pavement. This is helpful for engineers in runway maintenance agencies to efficiently understand the subgrade performance from HWD test result and make scientific decisions on M&R treatments such as improving the compactness and uniformity of soil foundation, continuously monitoring the properties of the soil base and timely repairing the damaged segment of subgrade. In application practice, proper calibration on the threshold values of  $\psi$  can be conducted according to the local safety management requirements, so as to achieve a better accuracy of estimation. The M&R experience can be obtained to provide advice for the design of runways in this region.

## Acknowledgements

This work was supported and the authors would like to acknowledge the National Key R&D Program of China (Grant No 2020YFB1600102), which funded this research.

## Funding

This work was supported by the National Key R&D Program of China under Grant No 2020YFB1600102.

## Author contributions

Guo-Guang Liu conceived the study and was responsible for the design and development of the data analysis.

Zhi-Wei Wu were responsible for data collection and analysis.

Guo-Guang Liu and Lei-Yang Pei were responsible for data interpretation.

Guo-Guang Liu and Lei-Yang Pei wrote the 1st draft of the article.

Guo-Guang Liu, Lei-Yang Pei and Zhi-Wei Wu read and approved the final article.

## Disclosure statement

The authors declare that they have no competing financial, professional, or personal interests from other parties.

## References

- Ahmed, A. W.; Erlingsson, S. 2017. Numerical validation of viscoelastic responses of a pavement structure in a full-scale accelerated pavement test, *International Journal of Pavement Engineering* 18(1): 47–59. <https://doi.org/10.1080/10298436.2015.1039003>
- Alkasawneh, W.; Pan, E.; Han, F.; Zhu, R.; Green, R. 2007. Effect of temperature variation on pavement responses using 3D multilayered elastic analysis, *International Journal of Pavement Engineering* 8(3): 203–212. <https://doi.org/10.1080/10298430601116741>
- Aydin, M. M.; Topal, A. 2019. Effects of pavement surface deformations on traffic flow, *Transport* 34(2): 204–214. <https://doi.org/10.3846/transport.2019.8631>
- Biancardo, S. A.; Abbondati, F.; Russo, F.; Veropalumbo, R.; Dell'Acqua, G. 2020. A broad-based decision-making procedure for runway friction decay analysis in maintenance operations, *Sustainability* 12(9): 3516. <https://doi.org/10.3390/su12093516>
- Chai, G. W.; Kelly, G. 2008. Characterization of LTPP pavements using falling weight deflectometer, in *6th International Conference on Road and Airfield Pavement Technology*, 20–23 July 2008, Sapporo, Japan, 1–9. Available from Internet: <http://hdl.handle.net/10072/23636>
- Chai, G. W.; Kelly, G.; Huang, T.-T.; Chowdhury, S. H.; Golding, A.; Manoharan, S. 2018. New approaches for modelling subgrade nonlinearity in thin surfaced flexible pavements, *International Journal of Pavement Engineering* 19(2): 122–130. <https://doi.org/10.1080/10298436.2016.1172706>
- Cunliffe, C.; Mehta, Y. A.; Cleary, D.; Ali, A.; Redles, T. 2016. Impact of dynamic loading on backcalculated stiffness of rigid airfield pavements, *International Journal of Pavement Engineering* 17(6): 489–502. <https://doi.org/10.1080/10298436.2014.993395>
- Dai, Y.; Zhong, Z.; Tong, P. 2003. Transient response of airport runway, *Key Engineering Materials* 243–244: 135–140. <https://doi.org/10.4028/www.scientific.net/kem.243-244.135>
- De Luca, M.; Abbondati, F.; Yager, T. J.; Dell'Acqua, G. 2016. Field measurements on runway friction decay related to rubber deposits, *Transport* 31(2): 177–182. <https://doi.org/10.3846/16484142.2016.1192062>
- Dong, Z.; Ma, X.; Shao, X. 2018. Airport pavement responses obtained from wireless sensing network upon digital signal processing, *International Journal of Pavement Engineering* 19(5): 381–390. <https://doi.org/10.1080/10298436.2017.1402601>
- El-Raof, H. S. A.; El-Hakim, R. T. A.; El-Badawy, S. M.; Afify, H. A. 2020. Structural number prediction for flexible pavements us-

- ing the long term pavement performance data, *International Journal of Pavement Engineering* 21(7): 841–855. <https://doi.org/10.1080/10298436.2018.1511786>
- Feng, J.; Zhang, L.; Gao, L.; Feng, S. 2018. Stability of railway embankment of China under extreme storms, *Environmental Geotechnics* 6(5): 269–283. <https://doi.org/10.1680/jenge.17.00043>
- Gopalakrishnan, K. 2008. Predicting capacities of runways serving new large aircraft, *Transport* 23(1): 44–50. <https://doi.org/10.3846/1648-4142.2008.23.44-50>
- Gopalakrishnan, K.; Thompson, M. R. 2006. Severity effects of dual-tandem and dual-tridem repeated heavier aircraft gear loading on pavement rutting performance, *International Journal of Pavement Engineering* 7(3): 179–190. <https://doi.org/10.1080/10298430600704232>
- ICAO. 2022. *Aerodrome Design Manual: Part 3 – Pavements*. Doc 9157. Part 3. 3rd edition. International Civil Aviation Organization (ICAO). Available from Internet: <https://store.icao.int/en/aerodrome-design-manual-part-3-pavements-doc-9157-part-3>
- Imran, S. A.; Barman, M.; Nazari, M.; Commuri, S.; Zaman, M.; Singh, D. 2016. Continuous monitoring of subgrade stiffness during compaction, *Transportation Research Procedia* 17: 617–625. <https://doi.org/10.1016/j.trpro.2016.11.116>
- Ioannides, A. M. 2006. Concrete pavement analysis: the first eighty years, *International Journal of Pavement Engineering* 7(4): 233–249. <https://doi.org/10.1080/10298430600798481>
- Ioannides, A. M. 1991. Theoretical Implications of the AASHTO 1986 nondestructive testing method 2 for pavement evaluation, *Transportation Research Record* 1307: 211–220. Available from Internet: <https://onlinepubs.trb.org/Onlinepubs/trr/1991/1307/1307-024.pdf>
- Jia, J.; Liu, H.; Wan, Y.; Qi, K. 2020. Impact of vibration compaction on the paving density and transverse uniformity of hot paving layer, *International Journal of Pavement Engineering* 21(3): 289–303. <https://doi.org/10.1080/10298436.2018.1464656>
- Khavassefat, P.; Jelagin, D.; Birgisson, B. 2016. The non-stationary response of flexible pavements to moving loads, *International Journal of Pavement Engineering* 17(5): 458–470. <https://doi.org/10.1080/10298436.2014.993394>
- Khoury, I.; Sargand, S.; Hatton, D. C. 2022. Impact of base type on performance of rigid pavement: a case study, *International Journal of Pavement Engineering* 23(3): 888–999. <https://doi.org/10.1080/10298436.2020.1778691>
- Kim, I. T.; Tutumluer, E. 2005. Unbound aggregate rutting models for stress rotations and effects of moving wheel loads, *Transportation Research Record: Journal of the Transportation Research Board* 1913(1): 41–49. <https://doi.org/10.1177/0361198105191300105>
- Lak, M. A.; Degrande, G.; Lombaert, G. 2011. The effect of road unevenness on the dynamic vehicle response and ground-borne vibrations due to road traffic, *Soil Dynamics and Earthquake Engineering* 31(10): 1357–1377. <https://doi.org/10.1016/j.soildyn.2011.04.009>
- Lin, J.-H. 2014. Variations in dynamic vehicle load on road pavement, *International Journal of Pavement Engineering* 15(6): 558–563. <https://doi.org/10.1080/10298436.2013.770512>
- Liu, G.; Niu, F.; Wu, Z. 2020. Life-cycle performance prediction for rigid runway pavement using artificial neural network, *International Journal of Pavement Engineering* 21(14): 1806–1814. <https://doi.org/10.1080/10298436.2019.1567922>
- Loizos, A.; Charonitis, G. 2004. Bearing capacity and structural classification of flexible airport pavements, *Journal of Transportation Engineering* 130(1): 34–42. [https://doi.org/10.1061/\(ASCE\)0733-947X\(2004\)130:1\(34\)](https://doi.org/10.1061/(ASCE)0733-947X(2004)130:1(34))
- Malla, R. B.; Joshi, S. 2008. Subgrade resilient modulus prediction models for coarse and fine-grained soils based on long-term pavement performance data, *International Journal of Pavement Engineering* 9(6): 431–444. <https://doi.org/10.1080/10298430802279835>
- Mshali, M. R. S.; Steyn, W. J. 2022. Effect of truck speed on the response of flexible pavement systems to traffic loading, *International Journal of Pavement Engineering* 23(4): 1213–1225. <https://doi.org/10.1080/10298436.2020.1797733>
- Papadopoulos, E.; Cortes, D. D.; Santamarina, J. C. 2016. In-situ assessment of the stress-dependent stiffness of unbound aggregate bases: application in inverted base pavements, *International Journal of Pavement Engineering* 17(10): 870–877. <https://doi.org/10.1080/10298436.2015.1022779>
- Papagiannakis, A. T.; Zelelew, H. M.; Muhunthan, B. 2007. A wavelet interpretation of vehicle-pavement interaction, *International Journal of Pavement Engineering* 8(3): 245–252. <https://doi.org/10.1080/10298430701309378>
- Park, H. M.; Chung, M. K.; Lee, Y. A.; Kim, B. I. 2013. A study on the correlation between soil properties and subgrade stiffness using the long-term pavement performance data, *International Journal of Pavement Engineering* 14(2): 146–153. <https://doi.org/10.1080/10298436.2011.633167>
- Rahim, A. M.; George, K. P. 2005. Models to estimate subgrade resilient modulus for pavement design, *International Journal of Pavement Engineering* 6(2): 89–96. <https://doi.org/10.1080/10298430500131973>
- Rameshkah, S.; Olounabadi, M. M.; Malekzadeh, P.; Meraji, S. H. 2020. Dynamic response analysis of viscoelastic pavement using differential quadrature element method, *International Journal of Pavement Engineering* 21(11): 1321–1335. <https://doi.org/10.1080/10298436.2018.1545091>
- Rushing, J. F.; Darabi, M. K.; Rahmani, E.; Little, D. N. 2017. Comparing rutting of airfield pavements to simulations using pavement analysis using nonlinear damage approach (PANDA), *International Journal of Pavement Engineering* 18(2): 138–159. <https://doi.org/10.1080/10298436.2015.1039007>
- Sangghaleh, A.; Pan, E.; Green, R.; Wang, R.; Liu, X.; Cai, Y. 2014. Backcalculation of pavement layer elastic modulus and thickness with measurement errors, *International Journal of Pavement Engineering* 15(6): 521–531. <https://doi.org/10.1080/10298436.2013.786078>
- Shi, Z.; Wang, K.; Zhang, D.; Chen, Z.; Zhai, G.; Huang, D. 2019. Experimental investigation on dynamic behaviour of heavy-haul railway track induced by heavy axle load, *Transport* 34(3): 351–362. <https://doi.org/10.3846/transport.2019.10325>
- Snehasagar, G.; Krishnanunni, C. G.; Rao, B. N. 2020. Dynamics of vehicle-pavement system based on a viscoelastic Euler-Bernoulli beam model, *International Journal of Pavement Engineering* 21(13): 1669–1682. <https://doi.org/10.1080/10298436.2018.1562189>
- Taheri, A.; O'Brien, E. J.; Collip, A. C. 2012. Pavement damage model incorporating vehicle dynamics and a 3D pavement surface, *International Journal of Pavement Engineering* 13(4): 374–383. <https://doi.org/10.1080/10298436.2012.655741>
- Toll, D. G.; Rahim, M. S. M.; Karthikeyan, M.; Tsaparas, I. 2019. Soil-atmosphere interactions for analysing slopes in tropical soils in Singapore, *Environmental Geotechnics* 6(6): 361–372. <https://doi.org/10.1680/jenge.15.00071>
- Vardon, P. J. 2015. Climatic influence on geotechnical infrastructure: a review, *Environmental Geotechnics* 2(3): 166–174. <https://doi.org/10.1680/envgeo.13.00055>

- Wang, H.; Li, M.; Garg, N. 2015. Airfield flexible pavement responses under heavy aircraft and high tire pressure loading, *Transportation Research Record: Journal of the Transportation Research Board* 2501: 31–39. <https://doi.org/10.3141/2501-05>
- Wang, H.; Li, M.; Garg, N.; Zhao, J. 2020. Multi-wheel gear loading effect on load-induced failure potential of airfield flexible pavement, *International Journal of Pavement Engineering* 21(6): 805–816. <https://doi.org/10.1080/10298436.2018.1511783>
- White, G. 2017. Limitations and potential improvement of the aircraft pavement strength rating system to protect airport asphalt surfaces, *International Journal of Pavement Engineering* 18(12): 1111–1121. <https://doi.org/10.1080/10298436.2016.1155122>
- Xue, W.; Weaver, E. 2015. Influence of tyre configuration on pavement response and predicted distress, *International Journal of Pavement Engineering* 16(6): 538–548. <https://doi.org/10.1080/10298436.2014.943206>
- Yang, J.-Q.; Cui, Z.-D. 2020. Influences of train speed on permanent deformation of saturated soft soil under partial drainage conditions, *Soil Dynamics and Earthquake Engineering* 133: 106120. <https://doi.org/10.1016/j.soildyn.2020.106120>
- Yang, S.; Chen, L.; Li, S. 2015. *Dynamics of Vehicle–Road Coupled System*. Springer. 327 p. <https://doi.org/10.1007/978-3-662-45957-7>